CHARACTERIZATION OF SURFACE ROUGHNESS OF LASER DEPOSITED TITANIUM ALLOY AND COPPER USING AFM

M. F. Erinosho[1,*], E. T. Akinlabi[1], O. T. Johnson[2]

[1]Department of Mechanical Engineering Science, University of Johannesburg, Auckland Park Kingsway Campus, Johannesburg, South Africa, 2006.
[2]Department of Mining and Metallurgical Engineering, University of Namibia, P.O. Box 3624, Ongwediva, Namibia.

*Corresponding author: **mutiuerinosho1@gmail.com**

Abstract

Laser Metal Deposition (LMD) is the process of using the laser beam of a nozzle to produce a melt pool on a metal surface usually the substrate and metal powder is been deposited into it thereby creating a fusion bond with the substrate to form a new material layer against the force gravity. A good metal laminate is formed when the wettability between the dropping metal powder and the substrate adheres. This paper reports the surface roughness of laser deposited titanium alloy and copper (Ti6Al4V + Cu) using the Atomic Force Microscopy (AFM). This AFM is employed in order to sense the surface and produce different manipulated images using the micro-fabricated mechanical tip under a probe cartridge of high resolution. The process parameters employed during the deposition routine determines the output of the deposit. A careful attention is given to the laser deposited Ti6Al4V + Cu samples under the AFM probe because of their single tracked layers with semi-circular pattern of deposition.

Keywords: AFM, LMD, microstructure, surface roughness, Ti6Al4V + Cu

1.0 Introduction

Titanium and its alloys are mostly gaining increased acceptance in aerospace, architecture, chemical processing, power generation, marine and offshore, sports and leisure, and transportation [1]. Due to the excellent biocompatibility among metallic materials, the alloy is also applied in the emerging biomedical applications [2, 3]. The atomic force microscopy (AFM) is referred to as the equipment that is used to view a three dimensional object in its full scale and down to the interpretation of the nanometer scale. This technique of viewing is applied to soft and hard synthetic materials as also the biological structures regardless of their opacity [4]. Nowadays, AFM is extensively used in many areas, for example, nanotechnology, industrial process control and materials science. Due to its versatility of the equipment, it is used to view nanoparticles objects and other molecular substances. With the advancement of the micro-fabricated cantilevers and the optical lever detection, AFM viewing has been improved technically [5]. The AFM is capable of doing specifically three operations. Firstly, it can measure the force that exists between the probe and the specimen under it. Secondly, it can form a three dimensional imaging profile as a result of the response of the probe on the specimen with respect to the force. This is accomplished by scanning the surface of the specimen. The third operation is controlling the force between the probe and the specimen in order to alter the properties of the sample [6].

2.0 Force determination and deflection of AFM cantilevers

For a high resolution images to be determined, the cantilever must have a sharp tip, high displacement sensitivity and high force sensitivity [5]. The cantilever is regarded as the most common sensor of the force interaction in AFM. Figure 1 shows a typical AFM cantilever with the tip pointing on the object to be scanned.

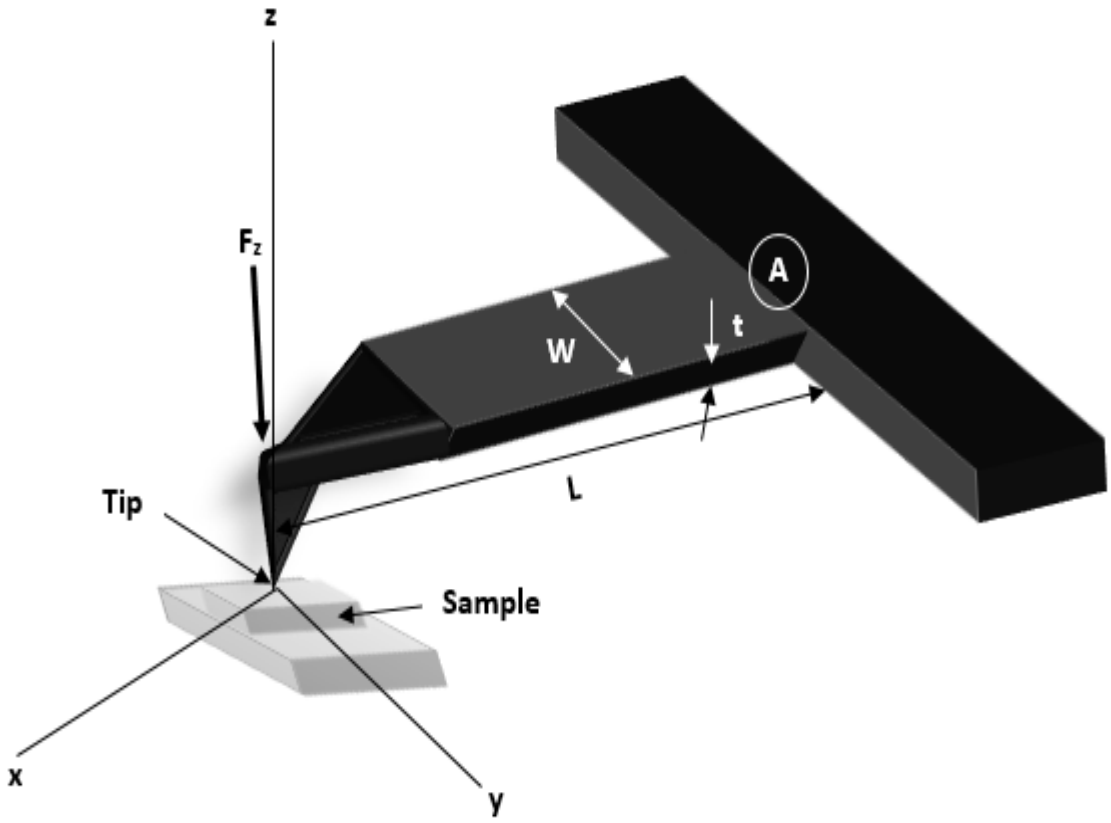

Figure 1: Schematic view of a cantilever

The relationship between the force (F) acting on the cantilever and the displacement at the tip (Δz) is needed in order to use the cantilever as a sensor. The cantilever is a beam with a length L, thickness t (where t <<L) and width w (where w << L). The probe's tip is directly in contact with the sample. According to Hooke's law, the force F_z acting the direction of z axis is proportional to the displacement Δz.

The reaction at point A as shown in equation (1) is

$$R_A = F_z . L \quad (1)$$

Where F_z acting the direction of z, L (mm) is the length of the cantilever

The maximum moment as shown in equation (2) is given by

$$M_A = [F_z . L^2]/2 \quad (2)$$

From the elementary beam theory we know that the deflection, Δz (mm) is given as

$$\Delta z = [F_z .L^3]/3.E.I \quad (3)$$

Where E (N/mm^2) is the elastic module and I (mm^4) is the moment of inertia. The moment of inertia of the beam section about the axis that passes through its centroid is given by

$$I = w \cdot t^3/12. \quad (4)$$

By substituting the moment of inertia I in equation (4) to equation (3), the force applied on the probe as shown in the z-axis can be written as

$$F_z = [\Delta z.E.w.t^3]/4.L^3 \quad (5)$$

Equation (5) is the expression of the applied force and for it to be determined, the elastic properties of the probe is needed to be know.

3.0 Surface roughness analysis with the AFM

The surface roughness of laser deposited Ti6Al4V + Cu sample (95 wt % Ti6Al4V + 5 wt % Cu) was analysed using the di3000 AFM equipment. The AFM is a surface-imaging system that uses a micro-fabricated mechanical tip under a probe cartridge. However, it is used for both two-dimensional (2D) and three-dimensional (3D) imaging of the surface topographies in the range between 100 μm – 0.1 nm. Before working on the AFM instrument, the TS-140 Vibration Isolation Table is switched ON to allow unlocking of the system. Secondly, the two AFM controllers are switched ON. The Nanoscope IIIa controller is switched ON first; then this is followed by the Dimension controller. The Central Processing Unit (CPU) is also turned ON. Before mounting the samples, the vertical deflection is set close to or approximately 0.00 V. The sum gauge below the detector is greater than 1.5, and this was followed according to the manual. The Auto Tune (AT) controls are engaged to get the correct resonance frequency. A target amplitude of 2.00 V and a peak offset of 0.00 % are set in the AT controls. The scan angle and X-Y offsets were set to zero (0); the sample/line was set to 256; and the slow scan axis was afterwards enabled.

4.0 Results and Discussion

The micrograph and the microstructure of the laser deposited Ti6Al4V + Cu sample deposited at a laser power of 1.2 kW and scanning speed of 0.3 m/min are shown in Figures 2 (a) to (d)

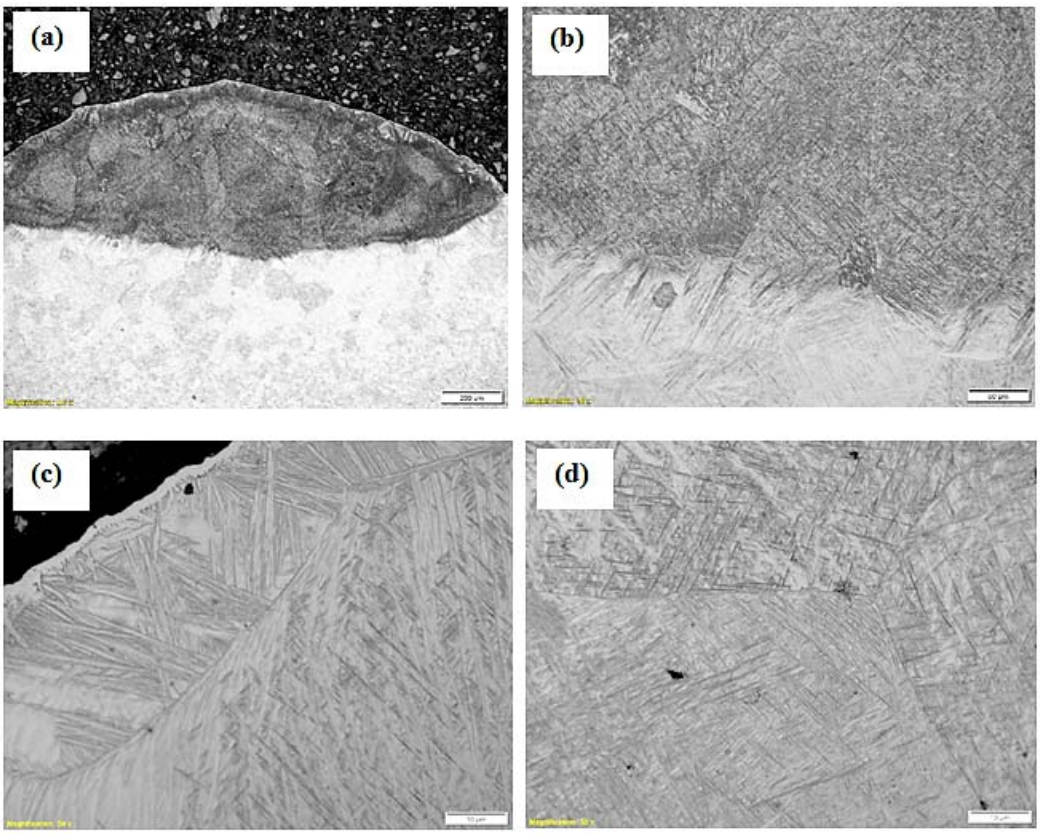

Figure 2: (a) Micrograph of the laser deposited samples at laser power of 1.2 kW and scanning speed of 0.3 m/min; (b) Microstructure of the samples between the deposit and the fusion zone; (c and d) Microstructures of the left towards the top and middle.

Figure 2 (a) shows the micrograph of the deposited sample; showing the deposited layer, the fusion zone and the heat affected zone. Macroscopic banding is observed in the deposited alloy and this can be attributed to the union of the (α+β) phase boundary [7]. Globular structures were also observed after the fusion zone. Figure 2 (b) shows the formation of basket weave-like structures and their formation are as a result of the cooling rate. Towards the fusion zone, the Widmanstätten structures are fused and became smaller with the evidence of α-martensitic phases. The faster cooling rate initiates the growth of the α-Ti phase and the Ti_2Cu phase [8]. Though, the Ti_2Cu phase is not observed in the microstructural analysis due to the 5 wt % of Cu used, although its presence has added to the properties of the deposited alloy.

The laser deposited sample was scanned under a probe cartridge attached with a silicon cantilever. At a resonance frequency, a drive signal positions the silicon cantilever into oscillation. A laser is deflected from the silicon cantilever onto the samples by a means of a positive sensitive photo-detector; and measures the topography. Figures 3 (a) to (c) show the measured height, the amplitude and the phase shift of the samples.

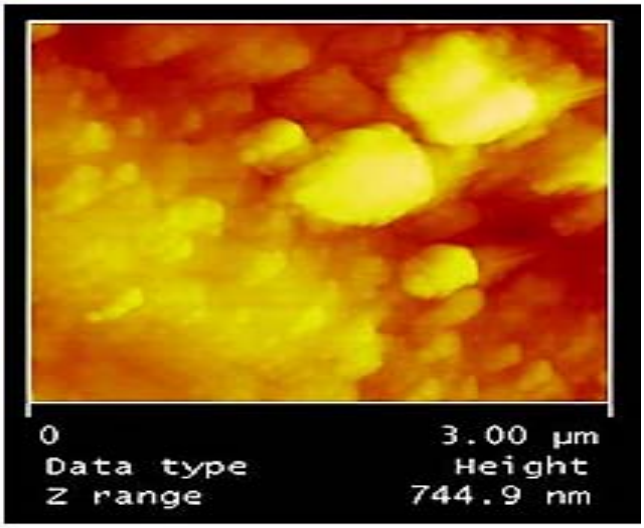

(a)

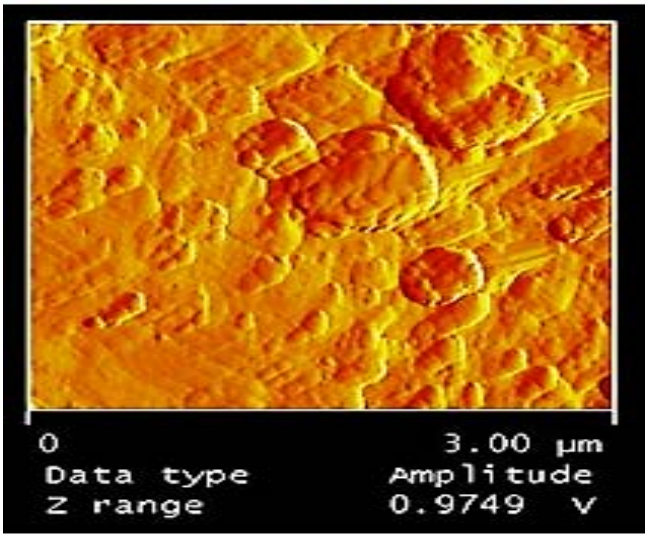

(b)

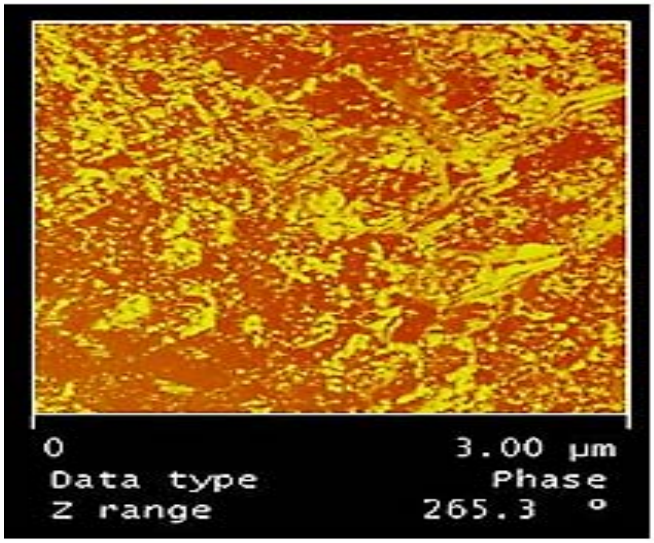

(c)

Figure 3: 2D surface topography of the laser deposited Ti6Al4V + Cu alloy showing the value of the height (nm), the amplitude (v) and the phase (^{o}).

The three 2D images are viewed simultaneously once a good scope trace is achieved. Alternately, the trend of the trace must be similar to the retrace in order to get a well captured image. The multi-colour images as observed in Figure 3 are mainly for viewing purposes. The contact between the tip and the sample is approximately constant [9]. The height of the surface is determined when the probe touches the surface of the testing sample. Hence, the vertical Z displacement can be measured via the feedback sensor. A good and perfect image is viewed when the surface topography is not too coarse. However, once the tip of the probe scans through the valley of the sample, no image is observed; and thus this drawback the Z position on the Trace Scope [10]. The Z-Range obtained for the height, the amplitude and the phase, as shown in the 2D view of Figures 3 are 744.9 nm, 0.9749 V and 265.3^{o}. Figure 4 shows the 3D surface topography of the laser deposited Ti6Al4V + Cu alloy.

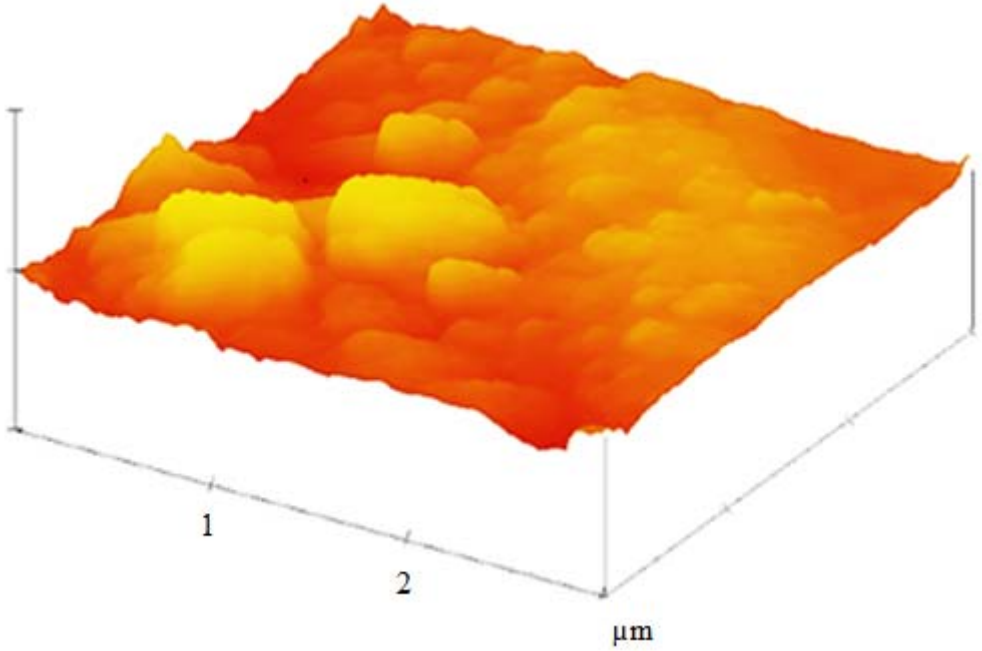

Figure 4: 3D surface topography of the laser deposited Ti6Al4V + Cu alloy.

From the sample image statistics, the arithmetical average of the absolute values of the profile height from the mean line, Ra, the mean, root mean square, Rms are 43.246 nm, 0.134 nm and 56.530 nm respectively. The surface roughness of laser deposited sample is important to analyse due to the deposition of powders of known particle size in microns on a solid plate. When analysing, the tip of the probe is always cautious of due to the coarseness and uneven nature of the surface. The crest and trough are asymmetrically distributed due to the different particle sizes and densities of the powders used. The deposited surface morphology is like a solidified mountain wave formed as a result of molten magma; and its formation depends on the process parameters used most especially the speed of scan and the laser power. In addition, the rate of surface cooling with the environment during solidification also determines the wave-like formed.

5.0 Conclusion

Laser deposition of metal is continuously gaining acceptance in the industries since the repair of difficult part can be achieved. The surface roughness of the deposited layer is importance and dependent on the engaged process parameters; and since it determines the semi finished topography. The surface topography of the laser deposited Ti6Al4V alloy with 5 wt % Cu was

successfully analysed. The relationship between the force acting on the cantilever and the deflection at the tip has been established. However, this force is determined once the elastic modulus of the cantilever is known. Before the dilution zone, the Widmanstätten structures were observed to fuse and became smaller with an indication of α-martensitic phases.

Acknowledgement

This work is supported by the National Research Foundation, Pretoria, South Africa and the National Commission on Research Science and Technology, Namibia.

Reference

[1] Leyens, C and Peters, M., (Eds.) "Titanium and Titanium Alloys", Fundamentals and Applications, Copyright, WILEY-VCH Verlag GmbH & Co. KGaA, Weinheim ISBN: 3-527-30534-3 (2003) pp 1-32.

[2] Moiseyev, V. N., "Titanium alloys: Russian aircraft and aerospace applications", CRC Press Taylor & Froes Group, (2006) pp 169-180.

[3] Lutjering, G., and Williams, J. C., "Titanium, Engineering Materials and processes", Springer, Second Edition, (2007) pp 1-449.

[4] Greg Haugstad, Overview of Atomic Force Microscopy. www. charfac.umn.edu/instruments/afm_introduction.pdf, 2012. Accessed 5 March, 2015

[5] Georg Fantner, Atomic Force Microscopy, Advanced Bioengineering Methods Laboratory, Ecole Polytechnique Federale De Lausanne.

[6] Wikipedia, Atomic Force Microscopy. https://en.wikipedia.org/wiki/Atomic-force_microscopy. Assessed 07, June, 2016.

[7] Erinosho, M. F., Akinlabi, E. T., and Pityana, S., "Influence of Scanning Speed and Energy Density on the Evolving Properties of Laser Deposited Ti6Al4V/Cu Composites", *Proceedings of the World Congress on Engineering (WCE)*, London, (2015), Vol. II, pp 715-719.

[8] Tsao, L. C., "Basic Electrochemical Behaviour of Ti_7Cu Alloys for Medical Applications", *Acta Physica Polonica*, A, 122(3), (2012) pp 561-564.

[9] Haugstad, G., "Overview of Atomic Force Microscopy": www.charfac.umn.edu/instruments/afm_introduction.pdf, (2012). Accessed 5 March, 2015.

[10] Mutiu . F. Erinosho, Esther T. Akinlabi, "Surface topography of laser metal deposited Ti6Al4V and Cu", Advance Engineering Materials, 2016 Wiley-VCH Verlag GmbH & Co. KGaA, Weinheim, (2016) pp 1-10.